

## DFT study on the adsorption mechanism of pulegone and pulegone oxide molecules in gas and aqueous phases as effective corrosion inhibitors in Molar Hydrochloric Acid.

Z.Faska<sup>1,2\*</sup>, L. Majidi<sup>1</sup>

<sup>1</sup> Laboratoire des substances Naturelles & Synthèse et Dynamique Moléculaire, Faculté des Sciences et Techniques, Université Moulay Ismail, Errachidia, Morocco.

<sup>2</sup> Centre Régional des Métiers de l'Éducation et de la Formation, Draa- Tafilalt, Errachidia, Morocco.

\* Corresponding author:

[faskacfi@yahoo.fr](mailto:faskacfi@yahoo.fr)

Received 12 Oct 2017,

Revised 25 Nov 2017,

Accepted 15 Feb 2018

### Abstract

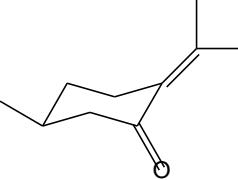
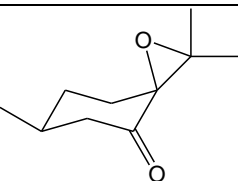
Quantum chemical calculations, based on DFT methods at B3LYP/6-311G(d;p) level of theory, were performed, by means of the G09 set of programs, on two p-menthane compounds. The objective of this work was to attempt to find relationships between the intrinsic electronic properties and inhibiting efficiencies of two p-menthane compounds, denoted P and PO, which have been previously studied experimentally as mild steel corrosion inhibitors in acidic medium. Based on these results, the Quantitative Structure–Activity Relationships (QSAR) studies allowed us to calculate the theoretic inhibitive efficiencies for this p-menthane compounds, of which the experimental study, was yet made. The structural electronic properties of the whole p-menthane compounds were investigated by means of number of global and local theoretical reactivity descriptors. The results showed that the electronic effect of the heteroatom and conjugate  $\pi$  double bonds markedly influenced the performance of the studied inhibitors.

**Keywords:** ; DFT; p-menthane; Corrosion inhibition; Fukui function; QSAR.

## 1. Introduction

Corrosion of mild steel is an inevitable process that produces deterioration of materials and their properties resulting in massive economic losses especially when it's occur in aggressive media like hydrochloric acid [1]. The study of corrosion process and their inhibition by organic inhibitors is a very active field of research [2]. Most efficient inhibitors are organic compounds containing electronegative functional groups and  $\pi$ -electrons in triple or conjugated double bonds [3]. Thus, the effectiveness of corrosion inhibitors is highly linked to their structural and electronic properties. Therefore, the use of theoretical study to correlate the electronic descriptors with the corrosion inhibition efficiency has been widely used in order to explain the experimental results, and also to elucidate the mechanism of corrosion inhibition process [4-5]. The aim of this work is to investigate structural relationships between the corrosion-inhibition efficiency and molecular properties of the surfactant molecules calculated at the density functional theory (DFT) levels. The study focuses on the prevention of steel corrosion in acidic medium and particularly on the corrosion- inhibition efficiency of the two p-menthane derivatives (Fig1). Calculated molecular properties, comprising the energy of the highest occupied molecular orbital ( $E_{\text{HOMO}}$ ), the energy of the lowest unoccupied molecular orbital ( $E_{\text{LUMO}}$ ), dipole moment ( $\mu$ ), and the total atomic charges (TAC), have been correlated to available experimental data[6]. Quantitative structure–activity relationship (QSAR) analysis[7] has been used to correlate the corrosion-inhibition activity of the studied molecules with the molecular structures. Multidimensional linear regression fits were used to determine relationships between the average corrosion-inhibition efficiency and the calculated molecular properties. The influence in the aqueous phase of the inhibitor molecules on the corrosion rate has been analyzed.

**Table 1:** Molecular structures, names and abbreviations of the studied p-menthane molecules

Inhibitor Formula	Name	Abbreviation
	p-menthan-5(8)-en-3-one (Pulegone)	P
	p-menthan-3-one Oxide (Pulegone Oxide)	PO

## 2. Materials And Methods

### 2-1. Quantum-chemical calculations methodology

In computational chemistry tools, the DFT offers the fundamentals for interpreting multiple chemical concepts used in different branches of Chemistry. In order to explore the theoretical-experimental consistency, quantum chemical calculations were performed with complete geometry optimizations using standard Gaussian-03 software package [8]. Geometry optimization were carried out by B3LYP functional at the 6-311G (d,p) basis set and at the density functional theory (DFT) level. Recently, Density functional theory (DFT) has been used to analyze the characteristics of the inhibitor/ surface mechanism and to describe the structural nature of the inhibitor in the corrosion process [9].

Furthermore, DFT is considered a very useful technique to probe the inhibitor/surface interaction as well as to analyze the experimental data. Since electrochemical corrosion takes place in liquid phase, and for a better approach of the experimental results, we used the Self-Consistent Reaction Field (SCRF) theory, with Tomasi's Polarized Continuum Model (PCM) [10], to include the effect of solvent in the computations. This approach models the solvent as a continuum of uniform dielectric constant ( $\epsilon$ ) and defines the cavity where the solute is placed as a uniform series of interlocking atomic spheres. The quantum chemical investigations were used to look for good theoretical parameters to be correlated with the inhibitive performance of the studied p-menthane derivatives. To do so, some of molecular properties, describing the global reactivity such as: the energy of the Highest Occupied Molecular Orbital, the energy of the Lowest Unoccupied Molecular Orbital, the energy gap ( $\Delta E$ ), the electrical dipole moment ( $\mu$ ), the Ionization Potential ( $IP$ ), the Electron Affinity ( $EA$ ), the electronegativity ( $\chi$ ), the global hardness ( $\eta$ ), and the fraction of transferred electrons ( $\Delta N$ ) were calculated. Other parameters describing the local selectivity of the studied molecules such as the local natural populations and the Fukui functions were also considered. In order to estimate some of the previous descriptors, the Koopmans' theorem was used [11] to relate the HOMO and LUMO energies to the  $IP$  and  $EA$ , respectively:

$$IP = -E_{HOMO} \quad EA = -E_{LUMO}$$

Then the electronegativity  $\chi$  and the global hardness  $\eta$  were evaluated, based on the finite difference approximation, as linear combinations of the calculated  $IP$  and  $EA$  [11]:

$$\chi = \frac{1}{2} (IP + EA) \quad \eta = \frac{1}{2} (IP - EA)$$

The fraction of transferred electrons  $\Delta N$  was calculated according to Pearson theory [12]. This parameter evaluates the electronic flow in a reaction of two systems with different electronegativities, in particular case; a metallic surface (Fe) and an inhibitor molecule.  $\Delta N$  is given as follows:

$$\Delta N = \frac{\chi_{Fe} - \chi_{inh}}{2 (\eta_{Fe} + \eta_{inh})}$$

where  $\chi_{Fe}$  and  $\chi_{inh}$  denote the absolute electronegativity of an iron atom (Fe) and the inhibitor molecule, respectively;  $\eta_{Fe}$  and  $\eta_{inh}$  denote the absolute hardness of Fe atom and the inhibitor molecule, respectively. In order to apply the eq. 5 in the present study, a theoretical value for the electronegativity of bulk iron was used  $\chi_{Fe} = 7\text{eV}$  and a global hardness of  $\eta_{Fe} = 0$ , by assuming that for a metallic bulk  $IP = EA$  because they are softer than the neutral metallic atoms [12].

The electrophilicity is a descriptor of reactivity that allows a quantitative classification of the global electrophilic nature of a molecule within a relative scale. Parr *et al* [13] have proposed electrophilicity index as a measure of energy lowering due to maximal electron flow between donor and acceptor. They defined electrophilicity index ( $\omega$ ) as follows.

$$\omega = \frac{\chi^2}{2\eta}$$

Fukui functions were computed since it provides an avenue for analyzing the local selectivity of a corrosion inhibitor [14]. Their values are used to identify which atoms in the inhibitors are more prone to undergo an electrophilic or a nucleophilic attack. The change in electron density is the nucleophilic  $f^+$  and electrophilic  $f^-$  Fukui functions, which can be calculated using the finite difference approximation as follows [15].

$$f^+ = q(N+1) - q(N)$$

$$f^- = q(N) - q(N-1)$$

where  $q(N)$ ,  $q(N+1)$  and  $q(N-1)$  are the electronic population of the atom in neutral, anionic and cationic systems.

## 2- 2 . Qsar study

Inhibitor concentrations and the calculated molecular properties were correlated with the average of the experimental inhibition efficiencies ( $E_{EXP}$  in %) using multidimensional linear regression, based on the QSAR approach, analyses performed with MATLAB program. Experimental measurements, were used to quantify the experimental corrosion-inhibition efficiency ( $E_{EXP}$  in %). The following proposed relation inhibition efficiency and quantum chemical index can be obtained:

$$E_{cal,i} = \sum_{j=1} (A_j X_j C_i + K) \times 100\% \quad \text{Eq (1)}$$

where ( $E_{CAL}$  in %) is the calculated inhibition efficiency,  $A_j$  constants are the linear regression coefficients determined by regression analysis,  $X_j$  is a quantum chemical index characteristic of molecule (j) and  $C_i$  denotes the experiment's concentration (i). In this work,  $X_j$  is constructed as a composite index of quantum chemical parameters  $E_{HOMO}$ ,  $E_{LUMO}$ ,  $\mu$ , and TAC. For the regression analysis, the molecular properties and  $C_i$  ranging from  $1\text{g.dm}^{-3}$  to  $10\text{g.dm}^{-3}$  are injected in Eq. (1). The  $A_j$  coefficients were obtained by fitting the HOMO-LUMO gaps, dipole moments ( $\mu$ ), and TAC to  $E_{EXP}$  using the Eq.(1) at different level of DFT.

## 3- Results And Discussion

### 3-1. Global molecular reactivity

The corrosion inhibitive process of organic molecules is defined as reaction involving the transfer of electrons between the inhibitor and the material surface. Hence, it can be explained according to Fukui's frontier molecular orbital theory, by the interaction between the HOMO and LUMO of the reacting species [31]. The calculated energies of the frontier orbital's and other parameters derived from these orbital's as well as the corresponding experimental inhibiting efficiencies of P and PO are collected in Table 2.

**Table 2.** Quantum chemical descriptors of the studied inhibitors at B3LYP/6-311G(d,p) in gas, G and aqueous, A phases and the inhibition efficiencies  $E_{exp}$  as given in [16].

Inhibitor	phase	$E_{tot}$ (eV)	$E_{HOMO}$ (eV)	$E_{LUMO}$ (eV)	$E$ (eV)	$\chi_{inh}$	$\eta_{inh}$	$\Delta N$	$\mu$ (Debye)	w	TAC (eV)	$E_{exp}$ (%)
P	G	-	-	-	5	3	2	0	2.81	2	-	8
		12678,99	6,19	0,99	.19	.59	.59	.65		.49	4.53	
	A	-	-	-	5	3	2	0	3.80	2	-	
		12678,50	6.41	1.11	.29	.76	.65	.61		.67	4.61	
PO	G	-	-	-	5.86	3	2	0	2.19	2	-	7
		14725,37	6,46	0,62		.54	.92	.59		.14	4.88	
	A	-	-	-	5.74	3	2	0	2.86	2	-	
		14724,69	6.55	0.81		.68	.87	.577		.36	4.95	

As  $E_{HOMO}$  is often associated with the electron donating ability of a molecule, high value of  $E_{HOMO}$  is likely to indicate the tendency of the molecule to donate electrons to an appropriate acceptor with lower energy empty molecular orbital. The calculated values of  $E_{HOMO}$  of the studied inhibitors in gas as well as in aqueous phases are presented in Table2.

The presence of the conjugated double bonds, as electron releasing through the mesomere (+M) effect in the pulegone molecule, should increase the electron density, enhancing its nucleophilicity [17]. On the other hand, the absence of conjugated double bonds in pulegone oxide, creates density deficiency, which will probably decrease their nucleophilicities. These assumptions explain the trend of the computed values of the EHOMO of the studied inhibitors. Indeed, the P displays the highest value in comparison with PO, which indicates that P is more likely to undergo nucleophilic attack more than the PO. The order of decreasing HOMO energy of the undertaken inhibitors is as follows:

$$EHOMO(P) > EHOMO(PO)$$

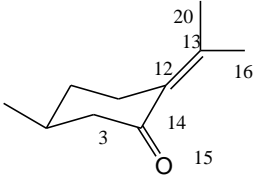
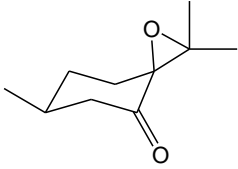
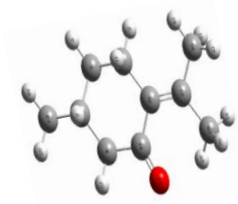
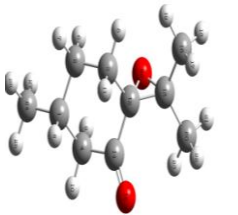
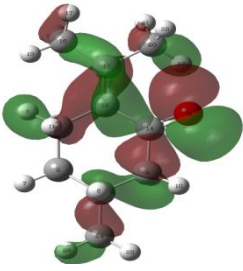
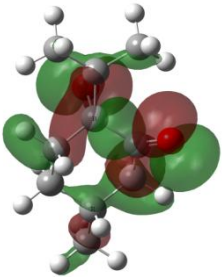
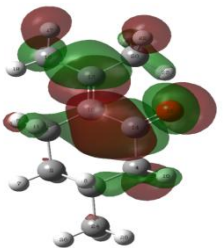
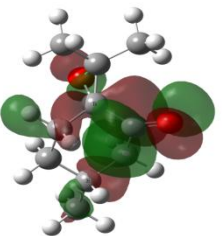
Likewise, the  $E_{LUMO}$  is associated with the electron accepting ability of the molecule, consequently, the low value of  $E_{LUMO}$  the high tendency to accept electrons from suitable electron donors. The values of the  $E_{LUMO}$  presented in Table 3 show that P in gas phase has the lowest  $E_{LUMO}$  when compared to PO which indicate better capability of P to accept electrons from the mild steel surface. This can also be explained by the electron deficiency in the pulegone molecule resulting of the conjugated bonds. The decreasing  $ELUMO$  can be ranked as follows:

$$ELUMO(P) < ELUMO(PO)$$

But in the aqueous phase (Table 3) we notice the inverse of what we have deduced in the case of the gaseous phase. This result can be explained by a slight stability of the pulegone in the aqueous phase.  $ELUMO(PO) < ELUMO(P)$

The gap between the EHOMO and ELUMO energy levels of the molecules is an important parameter as a function of reactivity of the inhibitor molecule towards the adsorption on the metallic surface. As  $\Delta E$  decrease the reactivity of the molecule increases leading to increase in the %IE of the molecule. Lower values of the energy difference will render good inhibition efficiency, because the energy to remove an electron from the last occupied orbital will be low [18]. Hard molecules have high HOMO-LUMO gap [19] and thus soft bases inhibitors are the most effective for metals [20]. The value of  $\Delta E$  indicated in table 1 show the following relation;  $P > PO$ , with a slight increase of  $\Delta E$  in the aqueous phase, which suggests that the inhibitor P in gas and aqueous phase has the lowest energy gap and highest reactivity in comparison to the other compound, could have better performance as corrosion inhibitor. The decreasing energy gap is as follows:  $\Delta E(P) < \Delta E(PO)$ . The dipole moment ( $\mu$ ) is a measure of the polarity of a covalent bond, which is related to the distribution of electrons in a molecule. However its relation to the efficiency of corrosion inhibitors is not yet well established and there is no agreement in the literature on the way of interpreting the trend of the dipole moment values in a set of corrosion inhibitors [21]. In fact, the computed values of the dipole moment do not allow any kind of interpretation with regards to the literature. From the computed results in aqueous phase (Table 3), we realize that the stabilization effect of the solvent is mainly noticed in the increase of the dipole moment  $d$  values in solution, which is probably a result of the polarization of the inhibitor molecules (solutes) by the solvent, leading to an increase in the charge separation in the molecules [22]. Absolute hardness is important property to measure the molecular stability and reactivity. It is apparent that the chemical hardness fundamentally signifies the resistance towards the deformation or polarization of the electron cloud of the atoms, ions or molecules under small perturbation of chemical reaction. A hard molecule has a large energy gap and a soft molecule has a small energy gap [46]. In our present study P with low hardness value 2.59(eV) in gas phase and 2.65(eV) in aqueous phase compared with PO (2.92 eV), have a low energy gap. Normally, the inhibitor with the least value of global hardness (hence the highest value of global softness) is expected to have the highest inhibition efficiency [23]. According to Lukovits's study [24], the fraction of transferred electrons describes the trend of electrons donation within a set of inhibitor. Generally, in the case of  $\Delta N$  less than 3.6, the inhibition efficiency increases with the increase in electron-donating ability to the metal surface. The obtained values of  $\Delta N$  reported in Table 3 are all below 3.6 and show that P presents the higher value of  $\Delta N$  (0.65 eV), which implies good disposition of this inhibitor to donate electrons to the mild steel surface.

The transferred electrons increase as follows:  $\Delta N(\text{PO}) < \Delta N(\text{P})$ . According to the definition, this index measures the propensity of chemical species to accept electrons. A good, more reactive, nucleophile is characterized by lower value of  $W$ ; and conversely a good electrophile is characterized by a high value of  $W$ . This new reactivity index measures the stabilization in energy when the system acquires an additional electronic charge  $\Delta N$  from the environment.

Inhibitor	Pulegone in gas phase	Pulegone Oxide in gas phase
Structure		
Structure optimisée		
HOMO		
LUMO		

**Figure 1.** The optimized molecular structures, and the HOMO and the LUMO electrons density distributions of the studied inhibitors computed at B3LYP/6-31G(d,p) level in gas phase.

### 3-2. Local molecular reactivity

Fukui functions compute local reactivity indices that makes possible to rationalize the reactivity of individual molecular orbital contributions. The condensed Fukui function and local softness indices allow one distinguish each part of the molecule on the basis of its distinct chemical behaviour due to the different substituted functional group.

The  $f_k^+$ , measures the changes of density when the molecules gains electrons and it corresponds to reactivity with respect to nucleophilic attack. On the other hand,  $f_k^-$  corresponds to reactivity with respect to electrophilic attack or when the molecule loss electrons. The calculated Fukui functions for the molecules P and PO are presented in Tables 3 and 4. According to fukui indices, C13 and C14 are the most reactive sites for nucleophilic attack and O15 is the site of electrophilic attack in the compound P in gas and aqueous phases. In the inhibitor PO, C13 is the site of nucleophilic attack and O15, O28 are the sites of electrophilic attack.

**Table 3.** Pertinent natural populations and Fukui functions of the studied inhibitor (pulegone **P**) calculated at B3LYP/6-31G(d,p) in gas (G) and aqueous (A) phases

inhibitor	phase	Atom N°	$q_N$	$q_{N+1}$	$q_{N-1}$	$f_k^+$	$f_k^-$
<b>P</b>	<b>G</b>	C12	-	-0,19610	-0,13159	-0,03234	-0,03217
		C13	0,16376	-0,10116	0,19862	<b>-0,20508</b>	-0,09470
		C14	0,10392	0,33969	0,58068	<b>-0,21819</b>	-0,02279
		O15	0,55789	-0,74555	-0,19913	-0,16772	<b>-0,37870</b>
		C16	-	-0,68760	-0,71277	0,02054	0,00463
		H17	0,57783	0,20707	0,27773	-0,03888	-0,03178
		H18	-	0,19919	0,28353	-0,04980	-0,03454
		H19	0,70814	0,21222	0,26442	-0,02912	-0,02308
		C20	0,24595	-0,68608	-0,70628	0,01765	0,00255
			0,24899				
	<b>A</b>		0,24134				
			-				
			0,70373				
		C12	-	-0,19612	0,03398	-0,03864	-0,19146
		C13	0,15748	-0,11916	0,25029	<b>-0,20549</b>	-0,16396
		C14	0,08633	0,34363	0,59102	<b>-0,23815</b>	-0,00924
		O15	0,58178	-0,78204	-0,35017	-0,18043	<b>-0,25144</b>
		C16	-	-0,69182	-0,73877	0,02402	0,02293
		H17	0,60161	0,20947	0,29688	-0,04477	-0,04264
		H18	-	0,20849	0,30026	-0,04591	-0,04586
		H19	0,71584	0,2222	0,2664	-0,02213	-0,02207
		C20	0,25424	-0,68971	-0,73806	0,02391	0,02444
			0,2544				
			0,24433				
			-				
			0,71362				



**Table 4.** Pertinent natural populations and Fukui functions of the studied inhibitor (pulegone oxide PO) calculated at B3LYP/6-31G(d,p) in gas(G) and aqueous (A) phases.

inhibitor	phase	Atom N°	q <sub>N</sub>	q <sub>N+1</sub>	q <sub>N-1</sub>	f <sub>k</sub> <sup>+</sup>	f <sub>k</sub> <sup>-</sup>
PO	G	C12	0,15533	0,15388	0,15407	-0,00145	0,00126
		C13	0,26255	0,23372	0,27297	-0,02883	-0,01042
		<b>C14</b>	0,57758	0,22557	0,61374	<b>-0,35201</b>	-0,03616
		<b>O15</b>	-0,54346	-	-0,22799	-0,22778	<b>-0,31547</b>
		C16	-0,69146	0,77120	-0,70894	0,00616	0,01748
		H17	0,23662	-	0,2685	-0,02935	-0,03188
		H18	0,26160	0,68530	0,27344	-0,02499	-0,01184
		H19	0,23525	0,20727	0,24605	-0,01397	-0,01080
		C20	-0,6918	0,23661	-0,71397	0,00503	0,02217
		<b>O28</b>	-0,55893	0,22128	-0,34621	-0,05493	<b>-0,21272</b>
				-			
				0,68680			
				-			
				0,61390			
	A	C12	0,15769	0,15305	0,19106	-0,00464	-0,03337
		C13	0,27289	0,24344	0,29071	-0,02945	-0,01782
		<b>C14</b>	0,59437	0,21411	0,63715	<b>-0,38026</b>	-0,04278
		<b>O15</b>	-0,57673	-	-0,24105	-0,24691	<b>-0,33568</b>
		C16	-0,69424	0,82364	-0,72176	0,00264	0,02752
		H17	0,24277	-0,6916	0,2771	-0,01651	-0,03433
		H18	0,25901	0,22626	0,27103	-0,01547	-0,01202
		H19	0,24161	0,24354	0,25601	-0,00992	-0,0144
		C20	-0,69448	0,23169	-0,72524	0,00349	0,03076
		<b>O28</b>	-0,58331	-	-0,38569	-0,05707	<b>-0,19762</b>
				0,69099			
				-			
				0,64038			

### 3-3. Linear regression analysis.

According to the slight difference values obtained through the calculation using these descriptors parameters, multidimensional linear least-square fit regression analysis was performed using MATLAB software. Several attempts to find correlations between calculated molecular properties of the inhibitor molecules and the corrosion-inhibition efficiency have been reported in the literature[25–29]. In the regression analysis, the inhibitor concentrations (Ci) and the obtained molecular properties in the quantum chemical calculations were correlated with the average of experimental inhibition efficiencies (E<sub>exp</sub>%). Three experimental methods, namely weight loss, impedance spectroscopy (EIS) methods and potentiodynamic polarization measurements were used[16]. The linear regression model shown in Eq. (1) quoted above gives the calculated corrosion-inhibitor efficiency (E<sub>CAL</sub> in %). The quality of.



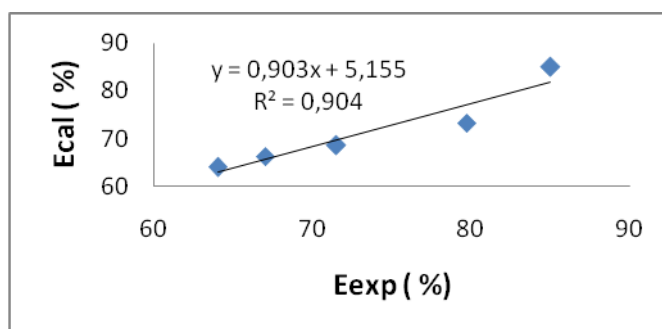


**Figure2.** Experimental inhibitor efficiencies of the pulegone molecule in gas phase measured at different concentrations as compared to fitted values from B3LYP calculations.

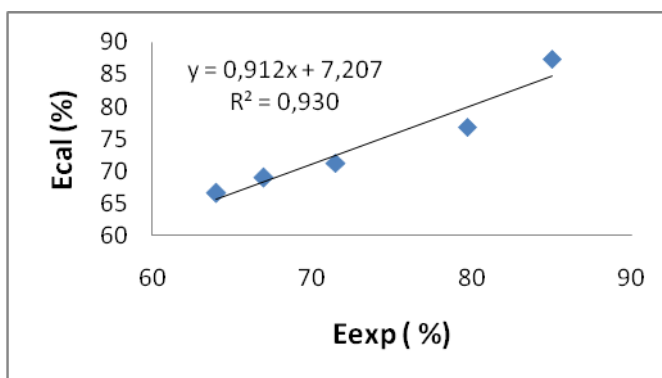


**Figure 3.** Experimental inhibitor efficiencies of the Pulegone molecule in aqueous phase measured at different concentrations as compared to fitted values from B3LYP calculations.

**Table 5.** Comparison of experimental ( $E_{EXP}$  in %) and calculated ( $E_{CAL}$  in %) corrosion-inhibition efficiencies of the *P*, and *PO* molecules as a function of the concentration (in  $g \cdot dm^{-3}$ ) using three computational levels[16].

Inhibitor	Concentration (g/l)	E <sub>cal</sub> (%)	E <sub>exp</sub> (%)
<b>Pulgone (P)</b>	<b>1</b>	64,00	64,00
	<b>2</b>	66,34	67,00
	<b>3</b>	68,67	71,50
	<b>4</b>	71,01	78,00
	<b>5</b>	73,35	79,70
	<b>10</b>	85,02	85,00
<b>Pulgone oxide (PO)</b>	<b>1</b>	56,72	50,00
	<b>2</b>	59,24	64,00
	<b>3</b>	61,76	67,00
	<b>4</b>	64,28	71,00
	<b>5</b>	67,80	75,00
	<b>10</b>	79,40	78,00

the fit depends of the high correlation coefficient,  $R^2$ . Then,  $R^2$  values close to one indicate that the investigated model satisfactorily reproduce experimental corrosion-inhibition efficiencies. The  $A_j$  coefficients were obtained by fitting all used descriptors to  $E_{EXP}$  using the Eq. (1) at different level of theory. Figure 2,3 shows the correlation between the experimental inhibition efficiency ( $E_{exp}\%$ ) and the calculated inhibition efficiency ( $E_{cal}\%$ ). The calculated and measured corrosion-inhibitor efficiencies are compared in Table 5. It can be seen from Figure 2 that the model illustrate good correlation with the experimental corrosion- inhibition efficiencies [(comparison between ( $E_{cal}\%$ ) and ( $E_{exp}\%$ ))] and the obtained  $R^2$  value is 0.90 in gas phase and 0.93 in aqueous phase. Thus, multidimensional regression analysis using calculated molecular properties can be useful for estimating corrosion-inhibition efficiencies with the goal to design new effective corrosion-inhibitor molecules. Thus, the aim is to estimate the efficiency of the inhibitor compounds by using several molecular properties and as the inhibition efficiency. A composite index consisting of more than one quantum chemical parameter is therefore used for characterizing the inhibition performance of the molecules

## 4- Conclusion

The corrosion-inhibition efficiency of the inhibitor molecules in HCl medium have been investigated computationally at DFT. The molecular properties obtained in the quantum chemical calculations are correlated to available experimental data for P, and PO in gas and aqueous phase. The calculations predict that P is a better corrosion inhibitor than PO. PCM calculations indicated that polar solvents slightly stabilize the inhibitor.

By using QSAR, we consider that the calculated quantum parameters study give a good correlation between calculated and experimental corrosion-inhibition data.

## REFERENCES

- [1] Z.El Adnani, M.Mcharfi, M.Sfaira, A.T. Benjelloun, M.Benzakour,M. Ebn Touhami, B.Hammouti, M.Taleb, *Int.J.Electrochem.Sci.*,7(2012) 3982-3993.
- [2] M. Bouayed, H. Rabba, A. Srhiri, J.Y. Saillard, A. Ban Bachir and A .Le Beuze, *Corros.Sci.*, 41(3) (1998) 501.
- [33] P.Udhayakala, T.V.Rajendiran, S.Gunasekaran, *J.Comput. Method.Mol.Design*, 2(1) (2012) 1
- [4] H. Elmsellem, A. Aouniti, M. Khoutoul, A. Chetouani, B. Hammouti, N. Benchat,, R. Touzani, M. Elazzouzi, *Journal of Chemical and Pharmaceutical Research*, 6(4) (2014) 1216
- [5] Z. El Adnani, M. Mcharfi, M. Sfaira, M. Benzakour, A.T. Benjelloun, M. Ebn Touhami, *Corros. Sci.*, 68 (2013) 223.
- [6] ] Z. Faska, A. Bellioua1, M. Bouklah, L. Majidi, R. Fihi, A. Bouyanzer, B. Hammouti,Monatsh Chem; 139 (2008) 1417–1422
- [7] C. Hansch, A. Leo, Substituent Constants for Correlation Analysis in Chemistry and Biology; John Wiley and Sons: New York, 1979.
- [8] ]. Frisch MJ, Trucks GW, Schlegel HB *et al.* Gaussian 03, Gaussian, Inc.: Pittsburgh PA, 2003.
- [9] ]. Lashkari M and Arshadi MR. *Chem Phys.*; **299** (2004) 131.
- [10] ]. W. Wang, W.J. Mortier *J. Am. Chem. Soc.*, 108 (1986) 5708.
- [11] ]. C.C. Zhan, J. A. Nichols, D.A. Dixon, *J.Phys.Chem. A*, 107 (2003) 4184.
- [12] ]. R.G. Pearson, *Inorg. Chem.*, 27 (1988) 734.
- [13] ] R.G. Parr, L. Szentpaly and S. Liu , *J.Am.Chem.Soc.*, , 121 (1999) 1922.
- [14] A.A. Siaka, N.O. Eddy, S.O. Idris and L. Magaji , *Research J. Appl. Sci.*, 6(7-120) (2011) 487.

- [15] M.A. Quijano, Pardav, A. Cuan, M.R. Romo, G.N. Silva, R.A. Bustamante, A.R. Lopez and H.H. Hernandez, *Int. J. Electrochem. Sci.*, **6** (2011) 3729.
- [16] Z. Faska, A. Bellioua1, M. Bouklah, L. Majidi, R. Fihi, A. Bouyanzer, B. Hammouti, *Monatsh Chem*; **139** (2008) 1417–1422
- [17] S.M. Soliman, *Comp. Theor. Chem.*, **994** (2012) 105.
- [18] M.K. Awad, M.S. Mustafa and M.M Abo Elnga, *J.Mol.Struct.*, **959**(1-3) (2010) 66.
- [19] X. Li, S. Deng, H. Fu and T. Li, *Electrochim. Acta*, **54**(2009) 4089.
- [20 ] M.A. Quraishi and R. Sardar, *J.Appl.Electrochem.*, **33**(12) (2003), 1163.
- [21 ] . N. Kovačević, A. Kokalj, *Corros. Sci.*, **53** (2011) 909.
- [22 ] . M.M. Kabanda, *Chem. Res. Toxicol.*, **25** (2012) 2153.
- [23 ] . Ebenso EE, David A. Isabirye and Nnabuk O.Eddy. *Int J Mol Sci*, **11** ( 2010) 2473.
- [24 ] . I. Lukovits, E. Kalman, F. Zucchi, *Corrosion*, **57** (2001) 3.
- [25] K. F. Khaled, K. Babic-Samardzija, N. Hackerman, *J. Appl. Electrochem.*, **34** (2004) 697.
- [26] J. Fang, J. Li, *J. Mol. Struct. (Theochem)*., **593** (2002)179.
- [27] O. Benali, L. Larabi, M. Traisnel, L. Gengembre, Y. Harek, *Appl. Surf. Sci.*, **253** ( 2007) 6130.
- [28] M. S. Masoud, M. K. Awad, M. A. Shaker, M. M. T. El-Tahaway, *Corros. Sci.*, **52**( 2010) 2387.
- [29] G. Bereket, E. Hur, C. O gretir, *J. Mol. Struct. (Theochem)*, **578** (2002) 79.